2018 European Control Conference (ECC)
June 12-15, 2018. Limassol, Cyprus

Hierarchical approach for Global Chassis Control*

Jean-Louis Bouvin[1,3], Emna Hamrouni[1,2,3], Xavier Moreau[1,3], André Benine-Neto[1,3], Vincent Hernette[2,3], Pascal Serrier[1,3] and Alain Oustaloup[1,3]

***Abstract*— This paper deals with the vehicle dynamics control and focuses on an illustrative example of an hierarchical approach for Global Chassis Control (GCC). This example, dealing with Global Suspension Control and especially with body control under driver solicitation in turns at a constant velocity enables the implementation of this hierarchical approach, composed of four levels (*Supervisor*, *Global Control*, *Control Allocation* and *Local Control*), improving the safety and the comfort of the passengers. Moreover, a comparison between two robust *Local* controller, a second generation CRONE and an H_∞ controller, designed with the same constraints, and whose performances are juxtaposed to those of the degraded operation mode of the active system (failure of the control), is presented. Results of the simultations using a 14 degrees-of-freedom (d-o-f) full vehicle model show a better body control using the hierarchical approach but comparable performances between the two robust controllers in the comfort operating domain.**

I. INTRODUCTION

Numerous studies concerning vehicle active roll control or rollover avoidance have already been developed. Roll control, corresponding to the body roll elimination, takes place, in most cases, in comfort operating domain and is ensured principally by active suspension [1]. Indeed, the indirect action of the suspensions on the lateral dynamics is sufficient to eliminate the body roll without acting on others degrees-of-freedom of the vehicle. For this purpose, several architectures have already been proposed. Authors in [2] proposes a structure with two nested control loops with an inner loop controller to cancel out the unwanted weight transfer and an outer loop controller to suppress both body vertical displacement and body roll angle. Furthermore, [3] presents a cascade structure with an upper level predictive anti-roll controller that uses road preview information for generating an optimal reference and a lower level sprung/unsprung mass motion controller that tracks the reference. In contrast, [4] proposes to use an active anti-roll bar as an actuator for roll control, but this system has a tendency to make the controlled vehicle exhibit an over-steer characteristic so that the controlled vehicle is drifted which means the loss of the maneuverability (but which can be maintained using integrated chassis control with Electronic Stability Control (ESC), Active Front Steering (AFS) and 4-Wheel Drive (4WD)). On the contrary, rollover avoidance takes place in the active safety operating domain so that all available actuators (steering wheel, traction, brakes, suspension) can be used at the same time, even if it acts on others degrees-of-freedom of the vehicle to prevent accidents [5].

With the rise of Advanced Driver-Assistance Systems (ADAS) such as Anti-lock Braking System (ABS), Electronic Stability Control (ESC) or Adaptive Cruise Control (ACC) a degradation of the general performance may occur in the absence of adequate coordination of the actuators. Indeed, as these systems were designed to operate individually reaching its own goal, the simultaneous action of one or several control systems acting, directly, indirectly or by coupling, on the global dynamics of the vehicle, can induce this degradation. It becomes clear that typical Global Chassis Control (GCC) architectures, such as centralized control, decentralized control or control by supervision [6], reach their limit in terms of flexibility for design and global vehicle performance.

Therefore, a hierarchical approach [7] is needed in order to allow the vehicle to identify the current situation (comfort, safety, etc.) and the according parametrisation of controllers, such that the different ADAS work harmoniously.

The hierarchical approach, composed of four levels (*Supervisor*, *Global Control*, *Control Allocation*, *Local Control*), allow to modify, as a function of the operating domain, the parametric state of the controllers (*Global* or *Local*) as well as those of the *Control Allocation*. Although this structure can be used with any control technique, this paper proposes, for *Global* and *Local* controllers, the use of CRONE control strategy, enabling the design of a robust controller by using fractional-order operators [8]–[10]. Moreover is designed a comparable H_∞ controller for the *Local Control* level.

This paper proposes the application of the hierarchical approach for the rolling dynamics regulation of a Citroën C4 Picasso, as shown in Fig. 1. The vehicle is equipped with a suspension system composed of passive metallic spring-damper units associated to actuators enabling the vehicle height regulation. These actuators can be choosen among different technologies such as pneumatic actuators, whose modeling has already been presented in [11], [12] considering the actuator of the pneumatic version of the Citroën C4 Picasso which acts as the spring when the leveling system is at rest, electromagnetic actuators, as existing in the Bose suspension [13], or hydropneumatic actuators as in the Hydractive suspension.

Fig. 1: Citroën C4 Picasso

Section 2 presents an anti-roll system based on CRONE control under hierarchical architecture whereas section 3 deals with the *Local* controllers design and section 4 provides, using a 14 degrees-of-freedom (d-o-f) full vehicle model, performance analysis relative to CRONE and H_∞ as *Local* controllers and juxtaposed with the degraded operation mode of the active system corresponding to a failure of the control. Finally, conclusions and perspectives are presented in section 5.

*This work took place in the framework of the OpenLab 'Electronics and Systems for Automotive' combining IMS laboratory and PSA Groupe company

[1]IMS, Univ. Bordeaux, CNRS, Bordeaux INP, 351 cours de la Libération, 33405 Talence cedex, France {firstname.lastname}@ims-bordeaux.fr

[2]PSA Groupe, 2 route de Gisy, 78943 Vélizy-Villacoublay, France {firstname.lastname}@mpsa.com

[3]OpenLab PSA Groupe - IMS Bordeaux

II. Hierarchical approach

From the particular case of roll control in curves at constant velocity, taken as an example, the four different levels composing this organization can be studied (from higher to lower level).

Thus, the diagram of the hierarchical approach selected for the GCC comprising four levels (*Supervisor*, *Global Control*, *Control Allocation* and *Local Control*) and applied to this example is presented in Fig. 2 with d_m being the measurable disturbances from the driver (steering wheel, pedals, etc.), d the non-measurable disturbances (slope, wind gust, etc.), Y_m the measurements from the vehicle, Y_r the *Local* outputs to control and U_{GC} and U_{LC} being, respectively, the input of the *Global* and of the *Local Control* and with the following notations:

- $X(t) = X^e + x(t)$: Variable (physical quantity) with X^e the equilibrium value of $X(t)$ (static part) and $x(t)$ the variation of $X(t)$ around X^e (dynamic part);
- $\tilde{X}(t)$: Measurement of $X(t)$;
- $\hat{X}(t)$: Estimation of $X(t)$;
- $\bar{X}(t)$: Desired value of $X(t)$;
- $X_{CG}(t)$: Physical quantity at the Center of Gravity (CG),
- $X_{nom}(t)$: Nominal value,

and the index $\{ij\}$ refering to the corresponding quarter of vehicle where $i = 1$ for front wheels and $i = 2$ for rear wheels, whereas $j = 1$ represents left wheels and $j = 2$ represents the right wheels.

Moreover, $X(s) = LT\{x(t)\}$ where LT denotes the Laplace Transform.

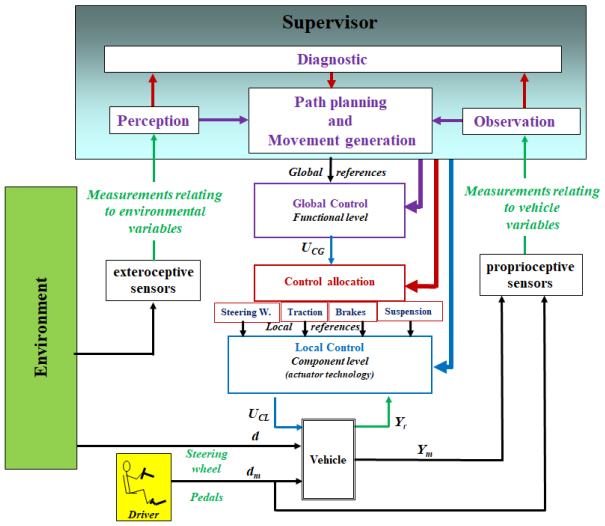

Fig. 2: Diagram of the hierarchical control

The following sections present, in more detail, each of the four levels composing the hierarchical approach for GCC in the particular case of roll control in curves at constant velocity.

A. Supervisor

This example focus on a stabilized turn at constant velocity $v_x = 50\ km/h$, such that the longitudinal acceleration $a_x = 0\ g$ and the lateral acceleration, at a steady state, $a_y = v_x^2/R$ ($|a_y| < 0.4\ g$) with R being the bending radius (m), so that it fits into the study of comfort and road behavior in the linear zone of the tires.

The rolling dynamics may be excited by the vehicle negotiating a curve. Due to lateral and gravitational accelerations, the external vertical loads are increased compared to internal ones, hence the generation of significant rolling torque causing the rolling motion.

As shown in Fig. 2, the *Supervisor* receives different measurements from the vehicle such as those of the vertical displacement $z_{2\_ij}(t)$ (m) and of the vertical velocity $v_{2\_ij}(t)$ (m/s) of each suspended mass, of the steering angle $\theta_v(t)$ (rad) (driver input) and of the roll rate at the center of gravity $\omega_{CG}(t)$ (rad/s) and defines, as a function of these measurements, the estimations of the rolling torque $C_{r0}(t)$ (Nm) and of the force generated by the passive elements of the suspension $f_{sp\_ij}(t)$ (N) with the following equations:

$$\hat{C}_{r0}(t) = H_{nom}\, M_{Tnom}\, \lambda_\theta\, \tilde{\theta}_v(t), \tag{1}$$

$$\hat{f}_{sp\_ij}(t) = k_{2\_ijnom}\, \tilde{z}_{2\_ij}(t) + b_{2\_ijnom}\, \tilde{\dot{z}}_{2\_ij}(t), \tag{2}$$

with λ_θ ($rad.m^{-1}.s^2$) being a constant fonction of the steering column gear ratio and of the inertial and geometrical parameters of the vehicle, H the height of the center of gravity (m), M_T the mass of the vehicle (kg) and b_{2_ij} and k_{2_ij} being the viscous coefficient of the damper (Ns/m) and the vertical stiffness of the spring (N/m).

As an illustration, Fig. 3 shows, considering $v_x = 50\ km/h$, the steering angle $\beta_v(t)$ (°) (variyng between 0 and 1.2°), the path generated (lateral displacement of the center of gravity $y_{CG}(t)$ (m) (varying from 0 to 24.7 m) as a function of its longitudinal displacement $x_{CG}(t)$ (m) (varying from 0 to 91.6 m)), the lateral acceleration $a_y(t)$ (m/s^2) (varying from 0 to 1.6 m/s^2 such that $|a_y| < 0.4\ g$) and the rolling torque $C_{r0}(t)$ (varying from 0 to 720 Nm) resulting from the steering wheel angle input $\theta_v(t)$ (varying from 0 to 15°).

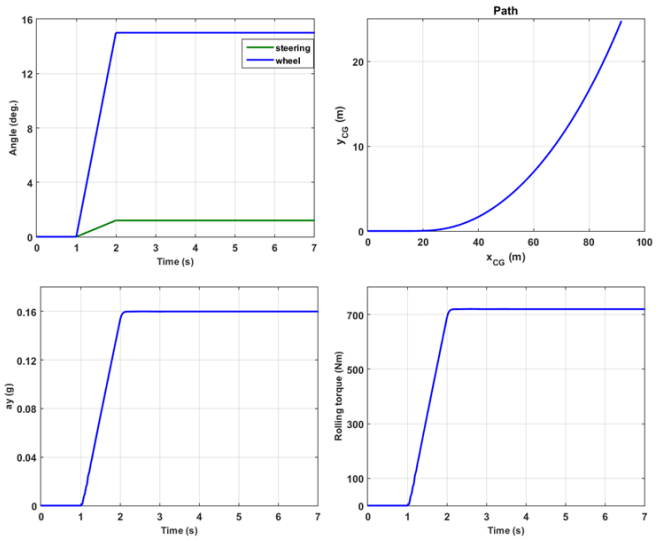

Fig. 3: Steering angle $\beta_v(t)$ (in green), path generated ($y_{CG}(t)$ as a function of $x_{CG}(t)$), lateral acceleration $a_y(t)$ and rolling torque $C_{r0}(t)$ resulting from the steering wheel angle input $\theta_v(t)$ (in blue)

B. Global Control

In this example, we focus on the roll rate control which causal form is defined as following:

$$\omega_{CG}(t) = \frac{1}{I_{xx}} \int_0^t C_{\Sigma_x}(\tau)\, \mathrm{d}\tau + \omega_{CG}(0), \tag{3}$$

where $C_{\Sigma_x}(t)$ (Nm) is the resulting torque caused by external torques applied to roll inertia I_{xx} $(kg.m^2)$ and defined by:

$$C_{\Sigma_x}(t) = C_{r0}(t) + C_{ar}(t), \tag{4}$$

with

$$C_{r0}(t) = H\, M_T\, a_y(t), \tag{5}$$

with $C_{ar}(t)$ being the anti-roll torque (Nm) defined with the four suspensions efforts $f_{s\_ij}(t)$ (N).

Moreover, $\bar{C}_{ar}(t)$ can be defined as following:

$$\bar{C}_{ar}(t) = C_{FF}(t) + C_{FB}(t), \tag{6}$$

with the anticipation feed-forward torque:

$$C_{FF}(t) = -\hat{C}_{r0}(t), \tag{7}$$

and the feed-back torque resulting from regulation with $K_{crone}(s)$ the transfer function of the $(Global)$ second generation CRONE controller:

$$C_{FB}(s) = -K_{crone}(s)\, \tilde{\Omega}_{CG}(s). \tag{8}$$

Thus, the block diagram corresponding to design of the *Global Control*, with $N(s)$ the sensor noise, is presented in Fig. 4.

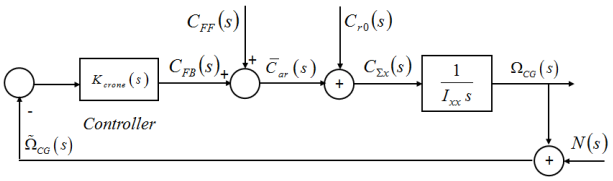

Fig. 4: Block diagram for the design of the *Global Control*

C. Control Allocation

Once the *Global Control* determined, the different efforts that will be generated by the four suspensions must be estimated. Thus, the relations enabling the transition between $\bar{C}_{ar}(t)$ and $\bar{f}_{s\_ij}(t)$ should be determined.

The expressions corresponding to the load transfers $f_{0\_ij}(t)$ at the level of the quarters vehicle is given by [14]:

$$f_{0\_ij}(t) = \frac{(-1)^{j-1}}{2l_i}\, C_{r0}(t) \tag{9}$$

with l_1 and l_2 being, respectively, the half-tracks of, respectively, the front and the rear axle (m).

Ideally, in order to control the car's body under driver inputs, the efforts generated by the four suspensions must be equal, and opposite, to the load transfers, so that:

$$f_{s\_ij}(t) = -f_{0\_ij}(t). \tag{10}$$

Therefore, and as part of the hierarchical approach, the desired values of the four suspensions are determined from $\bar{C}_{ar}(t)$ considering $l_1 = l_2 = l$, so that:

$$\bar{f}_{s\_ij}(t) = \frac{(-1)^{j-1}}{2l}\, \bar{C}_{ar}(t). \tag{11}$$

D. Local Control

Finally, at this level, the *Local Control* reference signals U_{LC} should be generated knowing the *Global Control* reference signals and the *Control Allocation*. In this example, the four suspension systems can be modeled by four quarter vehicle models for which the simplified model is presented in Fig. 5, considering a perfectly flat road so that the road vertical excitation $z_{0\_ij}(t) = 0\ m$ and the vertical displacement of the unsprung mass $z_{1\_ij}(t) \approx 0\ m$, with m_{2_ij} and m_{1_ij} being, respectively, the sprung and the unsprung masses (kg), k_{1_ij} and b_{1_ij} designating, respectively, the equivalent vertical stiffness (N/m) and viscous coefficient of the tire (Ns/m) and $f_{0\_ij}(t)$ modeling the load transfer (N) applied to the corresponding quarter vehicle.

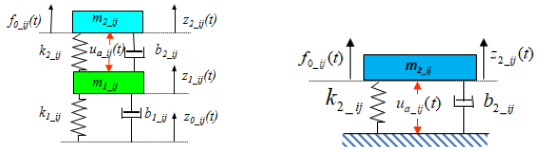

(a) For the validation (b) For the synthesis

Fig. 5: Quarter vehicle model

Therefore, $f_{s\_ij}(t)$ can be expressed as following:

$$f_{s\_ij}(t) = f_{sp\_ij}(t) + u_{a\_ij}(t), \tag{12}$$

with

$$f_{sp\_ij}(t) = f_{sC\_ij}(t) + f_{sR\_ij}(t), \tag{13}$$

$$u_{a\_ij}(t) = u_{FF\_ij}(t) + u_{FB\_ij}(t), \tag{14}$$

with $f_{sC\_ij}(t)$ and $f_{sR\_ij}(t)$ being, respectively, the effort developed by capacitive and resistive elements (N),

$$u_{FF\_ij}(t) = \bar{f}_{s\_ij}(t) + \hat{f}_{sp\_ij}(t), \tag{15}$$

and $u_{FB\_ij}(t)$ which can be considered according to the following strategy: 4 height regulations of the 4 quarter vehicle.

The schema for the design of the *Local Controller* is shown in Fig. 6 with $N_{ij}(s)$ the sensor noise (m). Moreover, and for symmetrical reasons, the two suspensions on a same axle are identical therefore only one controller should be designed for each axle.

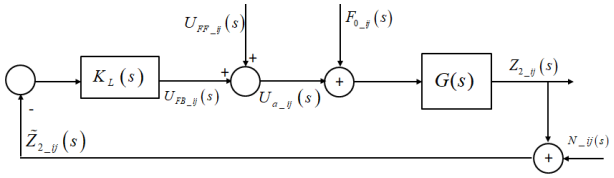

Fig. 6: Block diagram for the design of the *Local Control*

III. Controller Design

The requirements of the *Global Control* (Fig. 4) and *Local Control* (Fig. 6) systems are the following:

- for the *stability degree*: a resonant ratio of the complementary sensitivity function $Q_T \leq 3\ dB$;
- for the *rapidity*: the widest possible bandwidth, knowing that a minimal bandwidth at least four times wider than the driver bandwidth, whose superior limit is estimated near 2.5 Hz, is required;
- for the *precision at steady state*: a relative error lower than 1%;
- for the *control limit*: $\max\left|\bar{C}_{ar}\right| \leq 16000\ Nm$ or $\max\left|u_{a\_ij}\right| \leq 4000\ N$.

A. Global controller design

The CRONE control system design (CSD) methodology [8] is a frequency-domain approach (loop shaping), which has been developed since the 1980s [9], [10] and presents three approaches related to the three generations of CRONE control.

Considering the following transfer function of the plant $P(s)$, with $C_{\Sigma_x}(0)=0$ and $\omega_{CG}(0)=0$, which appears in (3):

$$P(s)=\frac{\Omega_{CG}(s)}{C_{\Sigma_x}(s)}=\frac{1}{I_{xx}\,s}, \tag{16}$$

being an integrator with an uncertain inertial parameter $I_{xx}\in[505,655]\ kg.m^2$, it can be deduced that the plant presents uncertainties which are only gain-like. Therefore, the second generation CRONE strategy can be used [8].

The optimal parameters of the open-loop transfer function and, a posteriori, of the second generation CRONE controller can be deduced, so that $n=1.5$ (medium frequency order), $n_l=2$ (low frequency order), $n_h=2$ (high frequency order), $r=0.77$ (gain variations around ω_u), $\beta_0=287.31$, $I_{xxnom}=580\ kg.m^2$, $K_0=1.67\times10^5\ kg.m^2.s^{-1}$, $a=b=10$, $\omega_l=7.15\ rad/s$ and $\omega_h=551\ rad/s$ (transitional low and high frequencies).

Thus, the rational controller transfer function

$$K_{crone}(s)=\frac{K_0}{s}\prod_{i=1}^{N}\left(\frac{1+\frac{s}{\omega_i'}}{1+\frac{s}{\omega_i}}\right) \tag{17}$$

can be determined, such that $K_0=\beta_0\,I_{xxnom}\,\omega_l^2$, with $N=4$ and after deducing ω_i and ω_i', using the methodology described in [15].

Bode and Black-Nichols diagrams of the open-loop with the CRONE controller previously designed, considering nominal $P_{nom}(s)$ and extreme plants $P_{min}(s)$ and $P_{max}(s)$ are plotted in Fig. 7. Thus, it can be deduced from these figures that the crossover frequency ω_u varies, according to the plant variations, from 74.0 rad/s to 88.1 rad/s but the highest resonant peak Q_T remains constant at 3.2 dB.

B. Local controller design

In this section, the design of the *Local* controller is presented using the feedback system presented in Fig. 6.

1) Plant definition: The transfer function of the plant is the following:

$$G(s)=\frac{1}{m_{2\_ij}\,s^2+b_{2\_ij}\,s+k_{2\_ij}}=\frac{G_0}{\left(\frac{s}{\omega_0}\right)^2+2\xi\,\frac{s}{\omega_0}+1}, \tag{18}$$

with the uncertain parameters m_{2_ij}, b_{2_ij} and k_{2_ij} which are different according to the studied quarter vehicle model ij, namely:

TABLE I: Uncertainties of the parameters

	Front axle ($i=1$)	Rear axle ($i=2$)
m_{2_ij} (kg)	$[393.2,479.0]$	$[270.7,513.5]$
b_{2_ij} (Ns/m)	$[1800,2200]$	$[1800,2200]$
k_{2_ij} (N/m)	$[22676,27715]$	$[26613,32527]$

Therefore, only one controller is designed, for each quarter vehicle, that is covering all the uncertainties of the parameters (for the two axles).

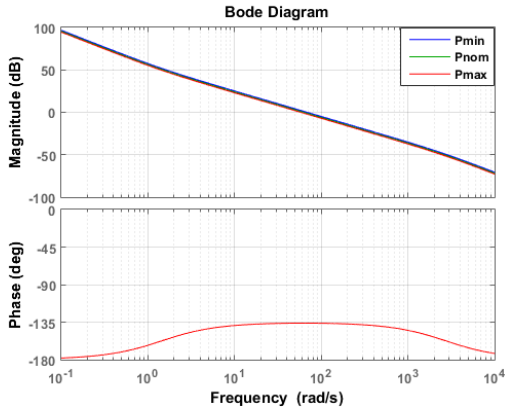

(a) Bode diagrams

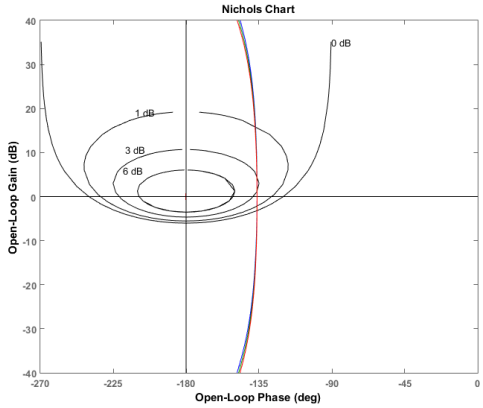

(b) Nichols diagram

Fig. 7: Open-loop Bode and Nichols diagrams for $P_{min}(s)$ (blue), $P_{nom}(s)$ (green) and $P_{max}(s)$ (red)

In this way, three transfer functions can be defined for the controller design: a nominal one and two extreme ones, namely:

$$\begin{cases} G_{nom}(s)=G(s,m_{2\_ijnom},b_{2\_ijnom},k_{2\_ijnom}) \\ G_{min}(s)=G(s,m_{2\_ijmin},b_{2\_ijmin},k_{2\_ijmin}) \\ G_{max}(s)=G(s,m_{2\_ijmax},b_{2\_ijmax},k_{2\_ijmax}) \end{cases}. \tag{19}$$

Given the specification defined previously, a CRONE controller is designed. In order to compare the performances with another robust controller, an H-infinity (H_∞) controller is designed such that it respects the same constraints on the sensitivity functions as represented in Fig. 9 with $S(s)$ the sensitivity function, $T(s)$ the complementary sensitivity function, $CS(s)$ the input sensitivity function and $GS(s)$ the input disturbance sensitivity function.

2) Second generation CRONE controller design: According to the specifications, ω_u is within a frequency range where the plant uncertainties are only gain-like so that a second generation CRONE controller can be designed. Then, using the same design as for the *Global* controller, the rational controller transfer function $K_L(s)$ can be determined using the methodology described in [15].

Thus, the optimal parameters of the open-loop transfer function and, a posteriori, of the second generation CRONE controller are $n=1.5$, $n_l=2$, $n_h=3$, $r=1.53$, $\beta_0=804.82$, $G_{0_{nom}}=7.45\times10^{-5}\ m/N$, $K_0=1.08\times10^7\ N/m$, $a=70$, $b=20$, $\omega_l=0.76\ rad/s$ and $\omega_h=1633\ rad/s$.

The Bode diagrams of the controller can be seen in Fig. 8.

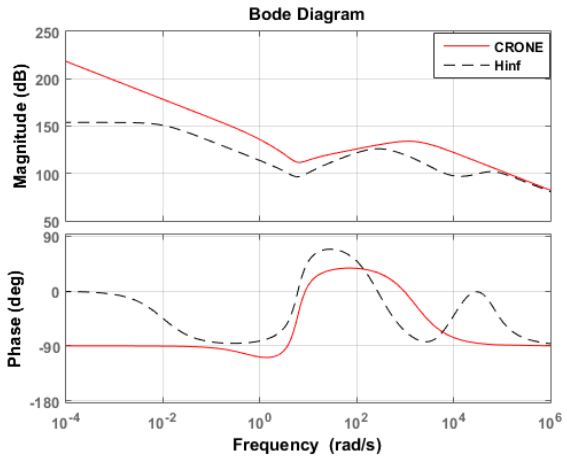

Fig. 8: Bode diagrams of the CRONE (solid red) and of the H_∞ (dashed black) controllers

3) H_∞ controller design: Using the robust control toolbox [16], the H_∞ controller is designed with the following methodology: the system specifications are, firstly, translated in terms of constraints for the sensitivity functions (taken into account for the design of the CRONE controller) and then approximated by transfer functions, of the lowest possible order, in order to avoid unnecessary complexity, while keeping a certain precision, so that each of the weightings can be then deduced.

The Bode diagrams of the H_∞ controller is also shown in Fig. 8. Moreover, the sensitivity functions $S(s)$, $T(s)$, $CS(s)$ and $GS(s)$, determined with the two controllers, and respecting the constraints previously defined according to the specifications are shown in Fig. 9.

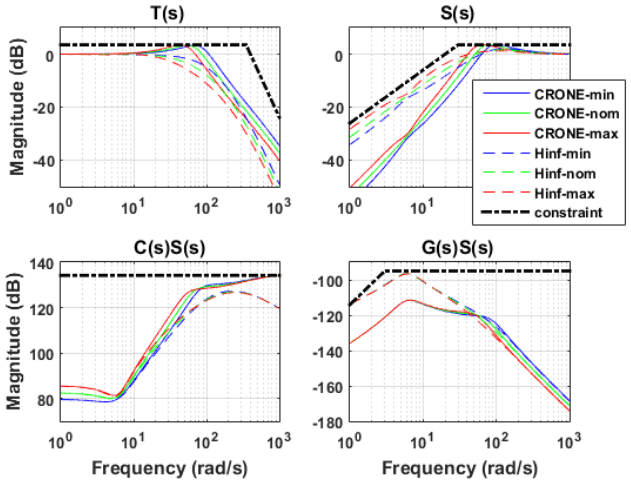

Fig. 9: Sensitivity functions $C(s)$, $T(s)$, $CS(s)$ and $GS(s)$

IV. Performance analysis

For all figures, unless otherwise stated, the curves corresponding to the CRONE controller are plotted in solid lines whereas those corresponding to the H_∞ controller are plotted in dashed lines and those corresponding to the degraded operation mode of the active system are plotted in dotted lines. Moreover, the curves corresponding, respectively, to the nominal $G_{nom}(s)$ and extreme plants $G_{min}(s)$ and $G_{max}(s)$ are plotted, respectively, in green, blue and red.

Using a 14 degrees-of-freedom (d-o-f) full vehicle model and according to the example previously defined, entering the corner enables the generation, at the *Local Control* level, of the four load transfers $f_{0\_ij}(t)$ presented in Fig. 10.(d) (where each subplot ij corresponds to the respective quarter of vehicle with line $i=1$ for front wheels and line $i=2$ for rear wheels, whereas column $j=1$ represents left wheels and column $j=2$ represents the right wheels).

Thanks to the hierarchical approach, and as a result of these load transfers, the four actuators generate, the efforts $u_{a\_ij}(t)$ represented in Fig. 10.(d) which are substantially rhe opposite of $f_{0\_ij}(t)$ in order to avoid the rolling motion, or to develop to anti-rolling torque necessary to compensate the rolling torque caused by the action on the steering wheel. Moreover, it can be seen than these efforts are comparable using the CRONE or the H_∞ controller.

Indeed, as seen in Fig. 10.(c) and Fig. 10.(b) , $u_{a\_ij}(t)$ is composed of a feed-forward part $u_{FF\_ij}(t)$ and a feedback part $u_{FB\_ij}(t)$ resulting from the regulation. Thus, due to the (low frequency) integral action, truncated for the H_∞ controller, the CRONE controller offers, thanks to its higher gain, a better rejection with $u_{FB\_ij}(t)$. Furthermore, this difference is completely compensated, in this operating domain, by the feed-forward parts $u_{FF\_ij}(t)$, which tend more slightly, for the H_∞ controller, to the final value (corresponding to the nominal configuration).

As a result for this example, the roll rate $\omega_{CG}(t)$ and the roll angle $\theta_{CG}(t)$ at the center of gravity, using the hierarchical approach with the CRONE or the H_∞ controller, remain close to zero. On the contrary, using the passive system, the maximum roll rate $\omega_{CG}(t)$ vary from 3.6 $^\circ/s$ to 5.9 $^\circ/s$ whereas the final roll angle $\theta_{CG}(t)$ vary from 2.9° to 4.1°, revealing the better body control under driver solicitations using the hierarchical approach.

V. Conclusion

In this article, the hierarchical approach for Global Chassis Control has been detailed and illustrated with a complete example for body control under driver solicitation in curves at a constant velocity as well as a comparison between a second generation CRONE and an H_∞ controller as *Local* controller (after translating the system specifications in terms of constraints for the sensitivity functions).

Thus, the hierarchical approach, composed of four levels (*Supervisor*, *Global Control*, *Control Allocation*, *Local Control*) allows to modify, as a function of the operating domain, the parametric state of the controllers (*Global* or *Local*) and of the *Control Allocation*. Moreover, it also enables the use of one or several actuators in order to act on the desired degrees-of-freedom of the vehicle without acting on the others and thus degrading the general performance.

In the example considered in this paper, located into the comfort operating domain, the use of this hierarchical approach offers an excellent body control under driver solicitation compared to the passive system, which can be illustrated with a roll angle and a roll rate really close to zero for the active system whereas the passive system just endures the rolling motion. Moreover, in this particular operating domain, the results obtained with the CRONE and the H_∞ controller are comparable.

Future work will be oriented on the study of other operating domains using the same approach. Indeed, in the active safety domains, the results obtained with the CRONE and the H_∞ controller may be relatively different. Moreover, working in other operating domains may require the action, not only on the suspension, but also on the steering wheels, the traction and the brakes.

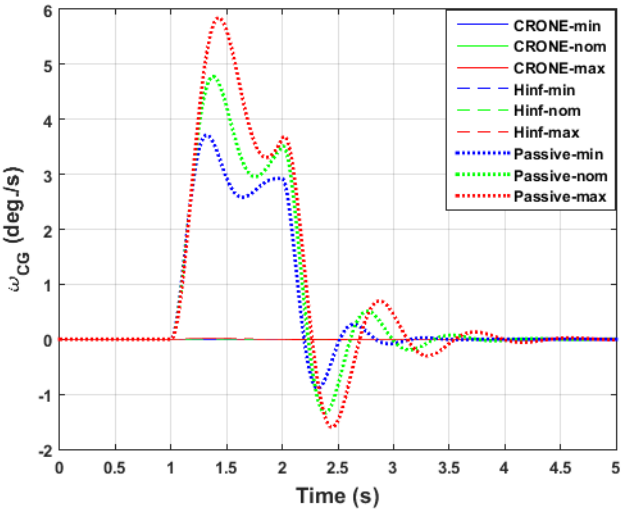

(a) Roll rate at the center of gravity $\omega_{CG}(t)$

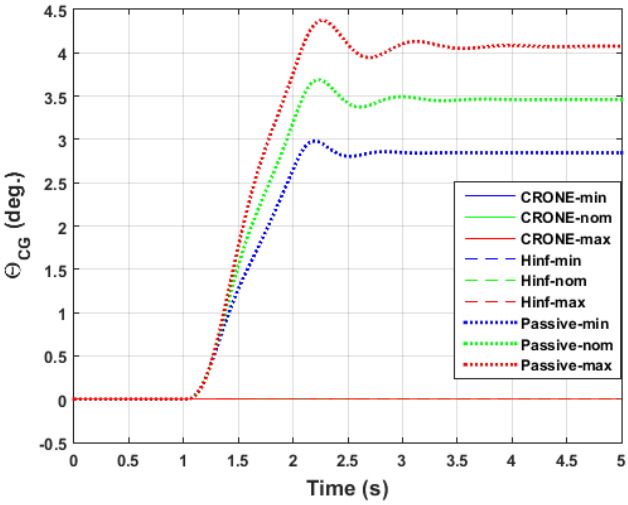

(b) Roll angle at the center of gravity $\theta_{CG}(t)$

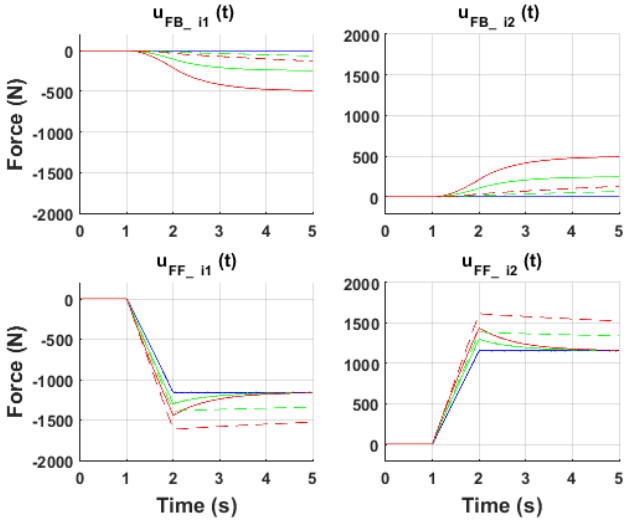

(c) Feed-back effort resulting from regulation $u_{FB\_ij}(t)$ and anticipation feed-forward effort $u_{FF\_ij}(t)$

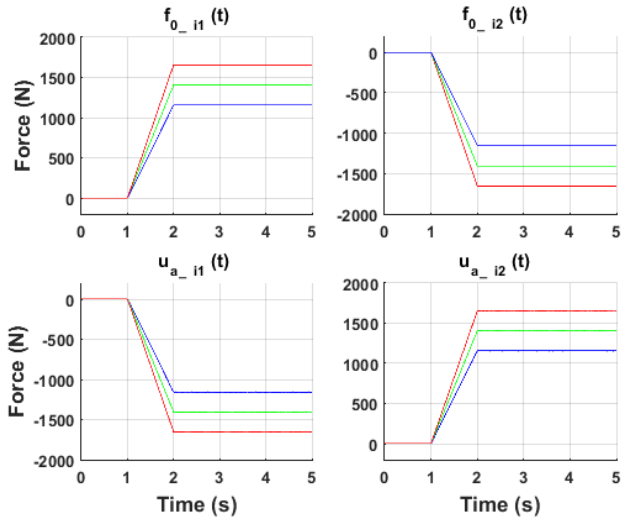

(d) Load transfers $f_{0\_ij}(t)$ and actuators efforts $u_{a\_ij}(t)$

Fig. 10: Time-related performances

REFERENCES

[1] Tseng, H. E., and Hrovat, D. (2015). State of the art survey: active and semi-active suspension control. *Vehicle system dynamics, 53(7), 1034-1062.*

[2] Kadir, Z. A., Hudha, K., Jamaluddin, H., Ahmad, F., and Imaduddin, F., Active roll control suspension system for improving dynamics performance of passenger vehicle. *Proceedings of 2011 International Conference on Modelling, Identification and Control, Shanghai, 2011, pp. 492-497.*

[3] Zhu, Q., and Ayalew, B. (2014, June). Predictive roll, handling and ride control of vehicles via active suspensions. *In American Control Conference (ACC), 2014 (pp. 2102-2107). IEEE.*

[4] Yim, S., and Yi, K. (2011, October). Design of active roll control system and integrated chassis control for hybrid 4WD vehicles. *In Intelligent Transportation Systems (ITSC), 2011 14th International IEEE Conference on (pp. 1193-1198). IEEE.*

[5] Chen, S. K., Moshchuk, N., Nardi, F., and Ryu, J. Vehicle Rollover Avoidance. *In IEEE Control Systems, vol. 30, no. 4, pp. 70-85, Aug. 2010.*

[6] Gordon, T., Howell, M., and Brandao, F. (2003). Integrated control methodologies for road vehicles. *Vehicle System Dynamics, 40(1-3):157-190.*

[7] Sename, O., Gaspar, P., Bokor, J. (2013). Robust Control and Linear Parameter Varying approaches: Application to Vehicle Dynamics. *Spinger, pp.397, 2013, LNCIS, n437.*

[8] Lanusse, P., Malti, R. and Melchior, P. (2013), CRONE control system design toolbox for the control engineering community: tutorial and case study, *Philosophical Transactions of the Royal Society of London A: Mathematical, Physical and Engineering Sciences*, The Royal Society, 371/1990.

[9] Oustaloup, A. (1983), Systèmes asservis linéaires d'ordre fractionnaire, Masson: Paris, France.

[10] Oustaloup, A. (1991), La commande CRONE, Hermès Editor: Paris, France.

[11] Bouvin, J.-L., Moreau, X., Benine-Neto, A., Oustaloup, A., Serrier, P. and Hernette, V. (2017). CRONE control of a pneumatic self-leveling suspension system, *IFAC-PapersOnLine, Volume 50, Issue 1, 2017, Pages 13816-13821.*

[12] Bouvin, J.-L., Moreau, X., Benine-Neto, A., Oustaloup, A., Serrier, P. and Hernette, V. (2017). CRONE body control under driver inputs through heave velocity regulation, *IEEE VPPC 2017*: Belfort, France.

[13] Brown, S.N. (2010). Active suspension system for vehicle, *2010.*

[14] Gillespie, T. (1992). Fundamentals of Vehicle Dynamics, *published by Society of Automotive Engineers, 1992,495 pages.*

[15] Oustaloup, A. (1995), La dérivation non-entière, Hermès Editor: Paris, France.

[16] Balas, G., Chiang, R., Packard, A., and Safonov, M. (2007). Robust Control Toolbox 3: User's Guide. Mathworks, Natick, MA.